Arthritis & Rheumatology
Vol. 0, No. 0, Month 2026, pp 1–13
DOI 10.1002/art.70123

American College of Rheumatology
Empowering Rheumatology Professionals

Tissue Damage in Rheumatoid Arthritis Is Genetically Linked to Low Peptidylglycine Alpha-Amidating Monooxygenase Activity in Synovial Fibroblasts

Kevin J. Sheridan, PhD,[1] Emma R. Dorris, PhD,[1] Maria Inês Pimenta, MSc,[1] Jemma Falkov, MSc,[1] Matthew Fisher, BSc,[2] Sam Pledger, MSc,[3] Hector Devey, MSc,[3] Munitta Muthana, PhD,[2] Denis C. Shields, PhD,[1] Richard E. Mains, PhD,[4] Betty A. Eipper, PhD,[4] Christopher D. Buckley, MB, PhD,[3] and Anthony G. Wilson, MB, PhD[1]

Objective. Both susceptibility to, and severity of, rheumatoid arthritis (RA) is associated with the rs26232 C allele. Our primary aim was to identify the biologic mechanism underlying this association.

Methods. Expression of surrounding genes was compared among rs26232 genotypes. Publicly available databases were used to correlate expression with RA inflammation and single-cell synovial distribution. Inhibition of gene expression and activity was achieved using small interfering RNA and a pharmacology agent and effects on RA synovial fibroblasts (RASFs) characteristics in vitro were assayed. The amidated secretome of synovial fibroblasts were characterized by mass spectrometry and enzyme-linked immunosorbent assay. Effects of amidated peptides on macrophage polarity were determined using an RASF–macrophage coculture module.

Results. rs26232 C is associated with low expression of peptidylglycine alpha-amidating monooxygenase (*PAM*) in multiple tissues including RASFs. Synovial *PAM* is highly expressed in RASFs but not immune cells, and levels are inversely correlated with synovial and systemic levels of inflammation. Inhibition of *PAM* in RASFs increased tissue-damaging activities such as invasiveness in vitro. The most abundant amidated peptides secreted by RASFs were adrenomedullin (ADM) and pro-ADM N-terminal peptide (PAMP). Incubation of RASFs with either peptide inhibited interleukin-6 (IL-6) and IL-8, increased transforming growth factor β production, and reduced invasiveness in vitro. Inhibition of amidation in an RASF–macrophage coculture model skewed the macrophages to proinflammatory MerTK$^-$ phenotypes.

Conclusion. Genetically determined low *PAM* reduces the anti-inflammatory and tissue-damaging activities of ADM and PAMP mediated by macrophages and RASFs, explaining the association of rs26232 C with RA severity.

INTRODUCTION

Rheumatoid arthritis (RA) is a chronic autoimmune disease characterized by inflammation in synovial joints that, if prolonged, results in cartilage and bone damage with resultant stiffness, pain, and reduced functional abilities. Pathogenesis involves both genetic and environmental risk factors. The severity of tissue damage in RA varies widely but has significant genetic input.[1] Of the more than 100 RA risk alleles identified in a genome-wide association study (GWAS), there is significant enrichment within immune-cell enhancers resulting in expression quantitative trait loci (eQTL).[2]

It has also been established that 24% of RA genetic risk arises from variants affecting gene expression in nonimmune cells such as RA synovial fibroblasts (RASFs).[3] These stromal cells are central mediators of inflammation and tissue damage in RA.[4] The

Supported by the Health Research Board (grant ILP-POR-2022-014). The Genotype-Tissue Expression Project was supported by the Common Fund of the Office of the Director of the NIH (commonfund.nih.gov/GTEx) and by National Cancer Institute, NIH; National Human Genome Research Institute, NIH; National Heart, Lung, and Blood Institute, NIH; National Institute on Drug Abuse, NIH; National Institute of Mental Health, NIH; and National Institute of Neurological Disorders and Stroke, NIH.

[1]University College Dublin Centre for Arthritis Research, Conway Institute, University College Dublin, Dublin, Ireland; [2]Department of Oncology and Metabolism, University of Sheffield, Sheffield, United Kingdom; [3]Kennedy Institute of Rheumatology, University of Oxford, Oxford, United Kingdom; [4]Department of Neuroscience, University of Connecticut Health Center, Farmington.

Additional supplementary information cited in this article can be found online in the Supporting Information section (https://acrjournals.onlinelibrary.wiley.com/doi/10.1002/art.70123).

Author disclosures are available at https://onlinelibrary.wiley.com/doi/10.1002/art.70123.

Address correspondence via email to Kevin J. Sheridan, PhD, at kevin.sheridan1@ucd.ie.

Submitted for publication September 1, 2025; accepted in revised form February 5, 2026.

invasive activities of RASFs in vitro are predictive of the rate of progression of joint damage.[5] The C allele of the single-nucleotide variant rs26232 is associated with both susceptibility to, and severity of, RA. The minor T allele is protective and occurs at a frequency of approximately 30%.[6–8] Cultured RASFs of this genotype are more invasive and produce higher levels of inflammatory cytokines and adhesion molecules compared with the CT genotype; although rs26232 is located within the first intron of *MACIR*, which has been shown to be involved in RASF-mediated tissue damage[9] and macrophage-directed inflammation,[10] the variant is not an eQTL for this gene.[11] This suggests that the link between rs26232 and RA may be related to the activity of another nearby gene.

Here, we show that rs26232 is an eQTL for the enzyme peptidylglycine alpha-amidating monooxygenase (PAM) that catalyzes the amidation of many secreted peptides, with low levels being associated with the RA risk C allele. Amidation replaces the carboxyl group at the C-terminal of a peptide with another amine group and is important for optimal activity of hormones and messenger molecules. In RA synovial tissue, *PAM* expression is predominantly restricted to RASFs. Inhibition of *PAM* results in greater tissue damage in vivo and in vitro, as well as shifting macrophages toward a proinflammatory phenotype. Lower amidation of two related secreted peptides, adrenomedullin (ADM) and pro-ADM N-terminal peptide (PAMP), is a mechanism underlying the association of rs26232 C allele with RA severity.

MATERIALS AND METHODS

Cell culture. RASFs were purchased from Sigma-Aldrich and maintained in RPMI medium, supplemented with 10% fetal bovine serum (FBS), penicillin (100 units/mL), and streptomycin (100 units/mL). The RNA for the 33 samples was taken from RASFs collected from patients in Ireland. RASFs were used between passages 3 and 8. For proteomic experiments, cells were grown in RPMI media without phenol red, supplemented with ascorbic acid (100 μM), $CuSO_4$ (50 μM), and insulin, transferrin, and selenium (Gibco, 41400-04). Peripheral blood mononuclear cells were isolated and macrophages differentiated as previously described.[11]

Recombinant amidated ADM (ADM-NH_2), glycine-extended ADM (ADM-Gly) and amidated PAMP (PAMP-NH_2) peptides were acquired from Phoenix Europe GmbH. Glycine-extended PAMP (PAMP-Gly) was custom ordered from GenScript Biotech. All peptides were used at concentration of 50 nM. 4-Phenyl-3-butenoic acid (PBA; Sigma, 155322) was used at a concentration of 1 μM. Tumor necrosis factor α (TNFα) was used at a concentration of 50 ng/mL. Lipopolysaccharide (LPS) was used at a concentration of 100 ng/mL. Hypoxia work was conducted at 3% O_2 using an Invivo$_2$ 400 workstation (Baker Ruskinn).

Flow cytometry. Fibroblast–macrophage coculture was seeded in RPMI at 2 × 10^5 cells/well per cell type and 4 × 10^5 cells/well for macrophage-only cultures. All media were treated with ascorbic acid and incubated at 3% O_2. Media was changed at 24 hours, and 1 μM PBA was added to the treatment wells in addition to ascorbic acid in both treatment (n = 3) and control (n = 3) wells. At 48 hours, cells were harvested for flow cytometry staining. Cells were washed in phosphate buffered saline (PBS) and incubated for 20 minutes in Live Dead (1:1,000) and Fc block (1:100) at 4°C. Samples were stained using the cell surface markers CD45, CD48, CD86, MerTK, and CD206 (1:100). Samples were centrifuged and washed with fluorescence-activated cell sorting (FACS) buffer (10% FBS in PBS). Samples were then fixed in 4% paraformaldehyde (PFA) for 20 minutes in the dark at room temperature and centrifuged, and the pellet was resuspended in 300 μL FACS buffer before being run on the BD Fortessa X20. Data were analyzed using FlowJo version 10.

Small interfering RNA knockdown in cell culture. Small interfering RNA (siRNA) targeting *PAM* (Dharmacon siGENOME SmartPool) or a nontargeting control siRNA (siNTC; Dharmacon siGENOME nontargeting pool 2) were transfected into RASFs at 30 nM using lipofectamine 2000 (Thermo Fisher) for 120 hours. siRNA targeting *PRG4* (siPRG4; Dharmacon siGENOME SmartPool) or siNTC (as above) were transfected into RASFs at 5 nM using lipofectamine 2000 for 72 hours. Knockdowns were confirmed using Western blot, and knockdown efficiency was calculated using densitometry.

Quantitative polymerase chain reaction. Messenger RNA (mRNA) was extracted from RASFs using Macherey-Nagel nucleospin mRNA kit (740955.50) and reverse-transcribed using Multiscribe reverse-transcriptase (Thermo Fisher, 4311235). Real-time polymerase chain reaction (PCR) was conducted on a Roche Lightcycler using Roche SYBR Green. Relative levels of total RNA for target genes (*PAM*, *GIN1*, *PPIP5K2*, and *MACIR*) were calculated using ΔΔCt method, with *HPRT1* used as a housekeeping gene. Primers used as listed in Supplementary Data Table 1.

Protein extraction and Western blotting. Cells were washed in cold PBS, then resuspended in N-PER Neuronal Protein Extraction Reagent (Thermo, 87792) containing protease inhibitor cocktail (Roche, 04693116001). Samples were placed on ice for 10 minutes, and the supernatant was collected after centrifugation (13,000 revolutions per minute for 10 minutes at 4°C). Total cellular protein was determined by means of the Bio-Rad DC protein assay (5000111). Protein samples were subjected to sodium dodecyl sulfate–polyacrylamide gel electrophoresis and then transblotted onto PVDF membranes. Membranes were blocked in 5% bovine serum albumin (BSA) or milk before overnight incubation at 4°C in primary antibody, then washed in

Tris buffered saline–Tween and incubated with the appropriate horseradish peroxidase-conjugated secondary antibodies for one hour at room temperature. Western blots were imaged on Vilber Fusion Fx 7 Edge. Antibody details are listed in Supplementary Data Table 2.

Invasion assay. RASFs were harvested, and 2×10^4 cells were resuspended in 500 μL of serum-free RPMI medium in the upper compartment of the Matrigel-coated inserts (Corning, 354480). The lower compartment was filled with complete media and incubated at 37°C for 24 hours. The upper surface of the insert was cleaned and then stained with 0.1% crystal violet. Five fields of invading cells were counted.

Apoptosis assay. Apoptosis was measured using CellEvent Caspase-3/7 Detection Reagent (Thermo Fisher, C10423). RASFs were seeded in triplicate in a 96-well plate at a density of 1,000 cells/well and incubated at 37°C overnight. Medium was then removed, and the cells were incubated in 2 μM CellEvent Caspase-3/7 Detection Reagent diluted in 5% FBS in PBS for 30 minutes at 37°C. Apoptosis was measured with an excitation/emission of 502/530 nm using a BMG FLUOstar Omega Platereader.

Proliferation assay. Proliferation was measured using bromodeoxyuridine (BrdU) proliferation enzyme-linked immunosorbent assay (ELISA; Roche, NC0947823). RASFs were seeded in triplicate in a 96-well plate at a density of 1,000 cells/well and incubated at 37°C overnight. BrdU labeling reagent was added to the cell media, and the plate was incubated at 37°C overnight. Cells were then fixed, incubated with peroxidase-conjugated anti-BrdU antibody, and substrate solution was added. Absorbance was measured at 370 nm using a BMG FLUOstar Omega Platereader.

Migration assay. RASFs were seeded into a 12-well plate at a density of 3×10^6 cells/well and incubated at 37°C overnight. Using a micropipette tip, a scratch was made in the cell monolayer. Medium was then removed, cells were washed with PBS, and fresh media was added. An image at zero hours was then captured, and the area of the wound was calculated using EPview software. The plate was then incubated at 37°C for 24 hours. A 24-hour image was then captured, and area of the wound was calculated as before. The percentage of wound closure was then calculated using the difference between the 0- and 24-hour wound areas.

Fluorescent microscopy. RASFs were seeded at a density of 1×10^6 cells/mL into a Millicell EZ Slide eight-well glass microscopy slide (Millipore, PEZGS0816) and incubated at 37°C overnight. Medium was removed, and cells were fixed with 4% PFA. Cells were permeabilized with 0.1% Triton X-100 and blocked with 2% BSA in PBS. Primary antibodies were incubated with cells at room temperature for two hours, followed by three washes with PBS. Fluorescent secondary antibodies and DAPI (1 μg/mL; Thermo Fisher, 62248) were incubated with cells at room temperature for one hour in the dark and washed as before. A glass coverslip was adhered to the cells with mounting medium. Images were captured using Zeiss LSM 800 Airy microscope using a 63× objective. Antibody details are listed in Supplementary Data Table 2.

Database searches. The GTEx Portal (https://www.gtexportal.org/home/) was used to compare mRNA expression in relation to rs26232 genotype. Correlation between PAM expression and clinical markers of inflammation was gathered from the Pathobiology of Early Arthritis Cohort database (https://peac.hpc.qmul.ac.uk/).[12] Single-cell RNA sequencing (RNAseq) data for the RA synovium were acquired from the Accelerating Medicines Partnership phase II (AMP2) RA project (https://immunogenomics.io/ampra2/).[13]

RNAseq. RASFs (n = 7) were transfected as previously described with siRNA targeting *PAM* (siPAM) or siNTC. mRNA was extracted from cultured cells using Macherey-Nagel nucleospin mRNA kit (740955.50). Reverse transcription and RNAseq were conducted externally by Eurofins Scientific. The differential expression analysis of the RNAseq data was performed using edgeR package.[14]

ELISAs. Human ADM (EK-010-01) and PAMP (EK-010-05) ELISA kits were purchased from Phoenix Europe GmbH, and samples were analyzed as per the kit protocol. Transforming growth factor β1 (TGFβ1; DY240-05), interleukin-6 (IL-6; DY206-05), IL-8 (DY208-05), and TNFα (DY210) ELISA kits were purchased from R&D Systems, and samples were analyzed as per the kit protocol. ELISA plates were analyzed using BMG FLUOstar Omega plate reader.

Half-life analysis. ADM-NH_2 and ADM-Gly were added to RPMI media (supplemented with 10% FBS) at a concentration of 50 ng/μL and incubated at 37°C for 1, 2, 4, 8, or 24 hours and then stored at –20°C. The samples were then separated in a 15% polyacrylamide gel and analyzed via Western blot and densitometry. Half-life was determined by plotting the relative density of the ADM-NH_2 and ADM-Gly time courses and using a best-fit line to determine the time at which density reached 50%.

Collagen-induced arthritis mice. Eight-week-old male DBA/1 mice (Harlan) were maintained under conventional animal housing conditions in a specific pathogen–free setting in accordance with the UK Animals (Scientific Procedures) Act, 1986. Mice were immunized intradermally into the base of the tail with 50 μg/50 μL immunization Grade Bovine Type II collagen solution

(Amsbio) previously emulsified in complete Freund's adjuvant (Merck). On day 21 after the initial collagen immunization, the mice were intradermally boosted with 50 μg/50 μL bovine type II collagen emulsified in Freund's incomplete adjuvant. Severity of disease was graded by using a scale of 0 to 2. Scoring was based on amount and severity of joint swelling, mobility, skin condition, general appearance, bodyweight, body condition, and grimace score. siRNA targeting murine *Pam* (Ambion In Vivo siRNA, assay ID s224168) and nontargeting control (Ambion In Vivo Negative Control 1) were purchased from Thermo Fisher. siPAM efficiency was tested in N2A (mouse neuroblastoma) cells before commencing the experiment (Supplementary Data Figure 1). Mice were treated with 1 mg/kg siRNA against murine PAM (n = 8), siNTC (n = 8), or the vehicle control (n = 8). Three intravenous injections were given on days 20, 22, and 24. Seven mice were given dexamethasone administered intraperitoneal (0.5 mg/kg). The drug was given daily from day 20 until day 49. Three DBA/1 mice were not induced to have arthritis and were not treated.

Mass spectrometry. Supernatant from RASFs was collected following a four-hour incubation. Peptides were isolated and concentrated from the supernatant using PTMScan Peptide Purification Kit (Cell Signaling Technology, 35741) and eluate dried down in a speed vacuum concentrator, resuspended in 2M urea and reduced and alkylated using dithiothreitol and iodoacetamide, then digested with trypsin overnight at 37°C. Resultant peptide mixtures were analyzed via a Thermo Fisher Q-Exactive mass spectrometer coupled to a Dionex RSLCnano. Protein identification was performed with Maxquant (version 2.4.2) using a custom modification to detect the 58-Da loss ($-H_2C_2O_2$) resulting from the amidation of glycine.

Statistical analysis. Statistical analyses were conducted using SPSS version 29. Anderson–Darling and Shapiro–Wilk tests for normality were performed for all variables. For parametric data, two-tailed paired Student's *t*-test was used for paired samples and unpaired Student's *t*-test was used to compare independent groups. Nonparametric data were analyzed using a Kruskal–Wallis test. Linear regression (of log-transformed data) was used to determine $t_{1/2}$. All experiments were performed at least three times unless otherwise stated. All hypothesis testing assumes an α level of 0.05. Data will be shared upon request.

RESULTS

Genetically determined low PAM expression in RASFs is inversely correlated with inflammatory activity in RA. We measured expression of genes within 300 kilobases of rs26232 in RASFs by quantitative PCR (Figure 1A) based on the regional block of strong linkage disequilibrium (LD) between *MACIR* and *PAM*. The C allele was associated with lower *PAM* mRNA levels but was not linked with expression of *MACIR*, *PPIP5K2*, or *GIN1* (Figure 1B). Interrogation of the online Genotype-Tissue Expression database (https://www.gtexportal.org/home/) revealed similar associations in multiple human tissues (Figure 1C). Although we did not find rs26232 to be a cis-eQTL for any other nearby genes in RASFs, multiple such associations were detected in the GTEx database (Supplementary Data Table 3). Analysis of the Pathobiology of Early Arthritis database (https://peac.hpc.qmul.ac.uk/) showed highest *PAM* mRNA expression in the fibroblast-rich compared with either the lymphoid- or myeloid-rich synovial pathotypes (Figure 1D); furthermore, levels were inversely correlated with both systemic markers of inflammation, including C-reactive protein (Figure 1E), erythrocyte sedimentation rate (Figure 1F), ultrasound-assessed joint inflammation including synovial thickness (Figure 1G), and power Doppler vascular signal (Figure 1H). Single-cell RNAseq of RA synovial tissue from the AMP2 (https://immunogenomics.io/ampra2/) revealed the highest expression in all RASF subtypes, low levels in endothelium, and minimal expression in leucocyte subsets (Figure 1I; Supplementary Data Figure 2).[13] Fluorescent microscopy analysis demonstrated PAM localized to the Golgi apparatus in RASFs but not the cilia (Supplementary Data Figure 3). These data suggest that genetically associated low *PAM* expression in RASFs is linked with RA.

Inhibition of PAM expression increases tissue-damaging activities of RASFs and inflammation in the collagen-induced arthritis model. To explore the biologic roles of PAM, we used siRNA to target expression in nine RASF lines (Figure 2A). This resulted in increased invasiveness (+18%, P = 0.001; Figure 2B) and proliferation (+37%, P = 0.002; Figure 2C) and reduced apoptosis (–24%, P = 0.0003; Figure 2D); compared to siNTC-treated cells, migration was unaffected (Figure 2E). To determine whether the effects of PAM inhibition were mediated directly by amidation, we used the PAM enzymatic domain inhibitor PBA.[15] Incubation of RASFs with PBA resulted in similar effects to siRNA-mediated inhibition of invasiveness in matched samples, confirming amidation as the underlying mechanism (Figure 2F).

Having determined that PAM is an inhibitor of the pathologic activities of RASFs in vitro, we hypothesized that inhibition would result in greater disease activity in vivo. The collagen-induced arthritis model was used to test this concept in *Pam*-knockdown mice. Deletion of *Pam* is embryonically lethal in mice, so an siRNA strategy to knock down *Pam* was employed to overcome this.[16] Mice were injected with collagen at 0 and 21 days and with siRNA (NTC or *Pam*) at 20, 22, and 24 days. At four and five weeks post-immunization, the mean clinical score was significantly more severe in the mice deficient of *Pam* compared with mice treated with siNTC (P = 0.004; Figure 2G).

In RASFs inhibition of *PAM* expression resulted in increased levels of 1,242 transcripts, whereas 1,253 were decreased compared with siNTC-treated cells (Figure 2H), including genes linked

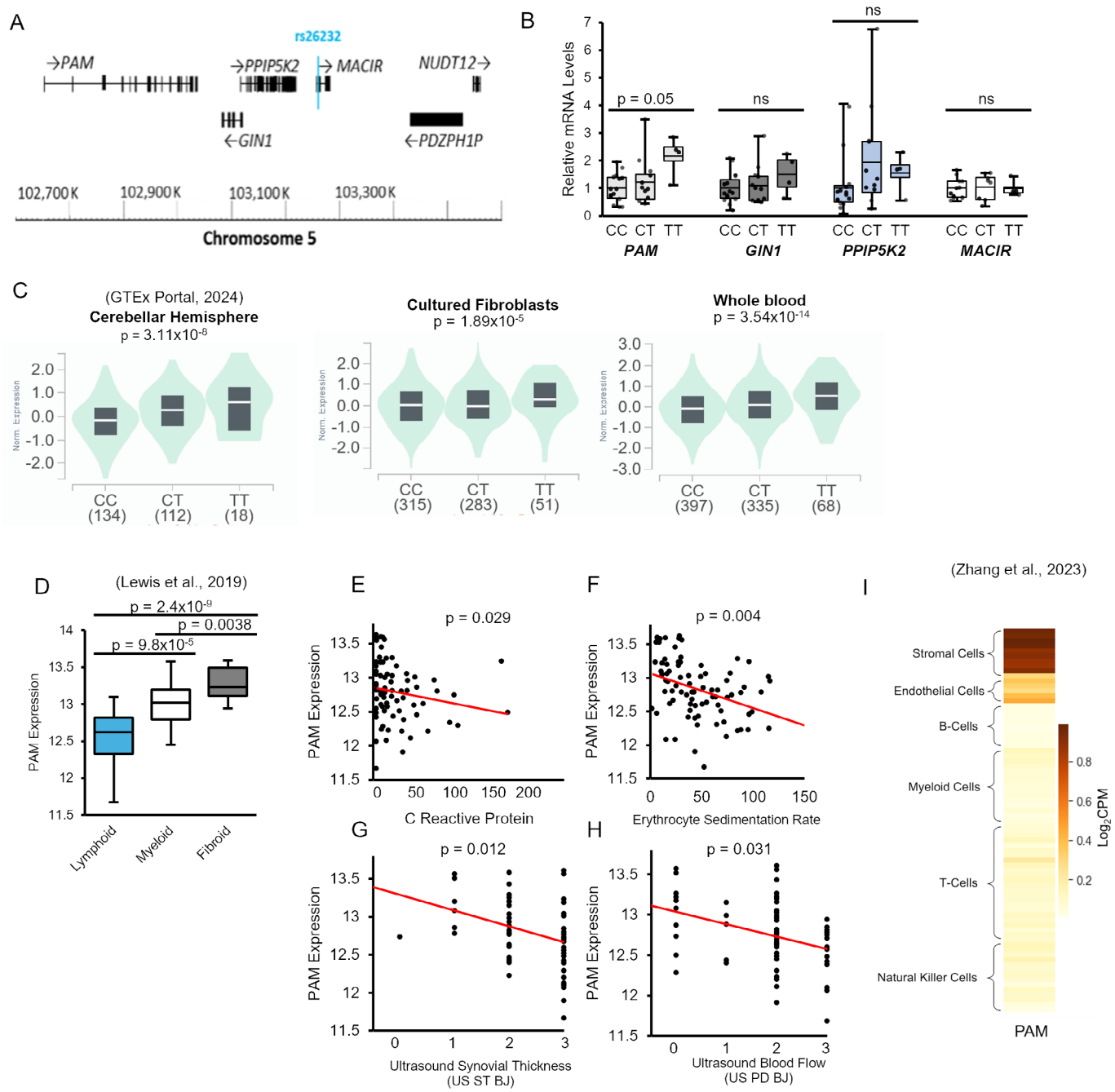

Figure 1. Relationship among rs26232 genotype, peptidylglycine alpha-amidating monooxygenase (PAM) expression, and rheumatoid arthritis (RA). (A) Annotation of genes in the locality of rs26232 (located within the first intron of *MACIR*). (B) Relative expression levels of *MACIR*, *PAM*, *GIN1*, and *PPIP5K2* in RA synovial fibroblasts (n = 33) by rs26232 genotype (CC, CT or TT). Kruskal–Wallis test was performed. (C) Association of rs26232 genotypes with PAM messenger RNA (mRNA) levels in human dermal fibroblasts, cerebellum, and whole blood in GTEx data. Rheumatoid synovial PAM mRNA levels and clinical activity in the Pathobiology of Early Arthritis study data (D) levels correlate with pathotype and inversely with measures of systemic inflammation, (E) C-reactive protein, (F) erythrocyte sedimentation rate, and ultrasound (US)-assessed synovitis including (G) synovial thickness (ST) and (H) blood flow. (I) Single-cell RNA sequencing in Accelerating Medicines Partnership phase II data showing subsets for cell lineages within the synovium. This reveals high level expression in all fibroblast subtypes with lower levels in endothelial cells and minimal expression in leucocytes. BJ, biopsy joint; CPM, counts per million; ns, not significant; PD, Power Doppler.

with proliferation, apoptosis, and invasion (Figure 2I). Of note was the reduced expression of *PRG4* (lubricin; $\log_2$ fold change –3.01, false discovery rate [FDR] $P = 1.06 \times 10^{-71}$; Figure 3F; Supplementary Data Table 4). PRG4 is a major constituent of synovial fluid, ensuring low frictional resistance in joints,[17] and has anti-inflammatory actions including reducing inflammatory cytokine–induced RASF proliferation.[18] PRG4 also regulates the balance of synovial macrophage subtypes, promoting a higher ratio of

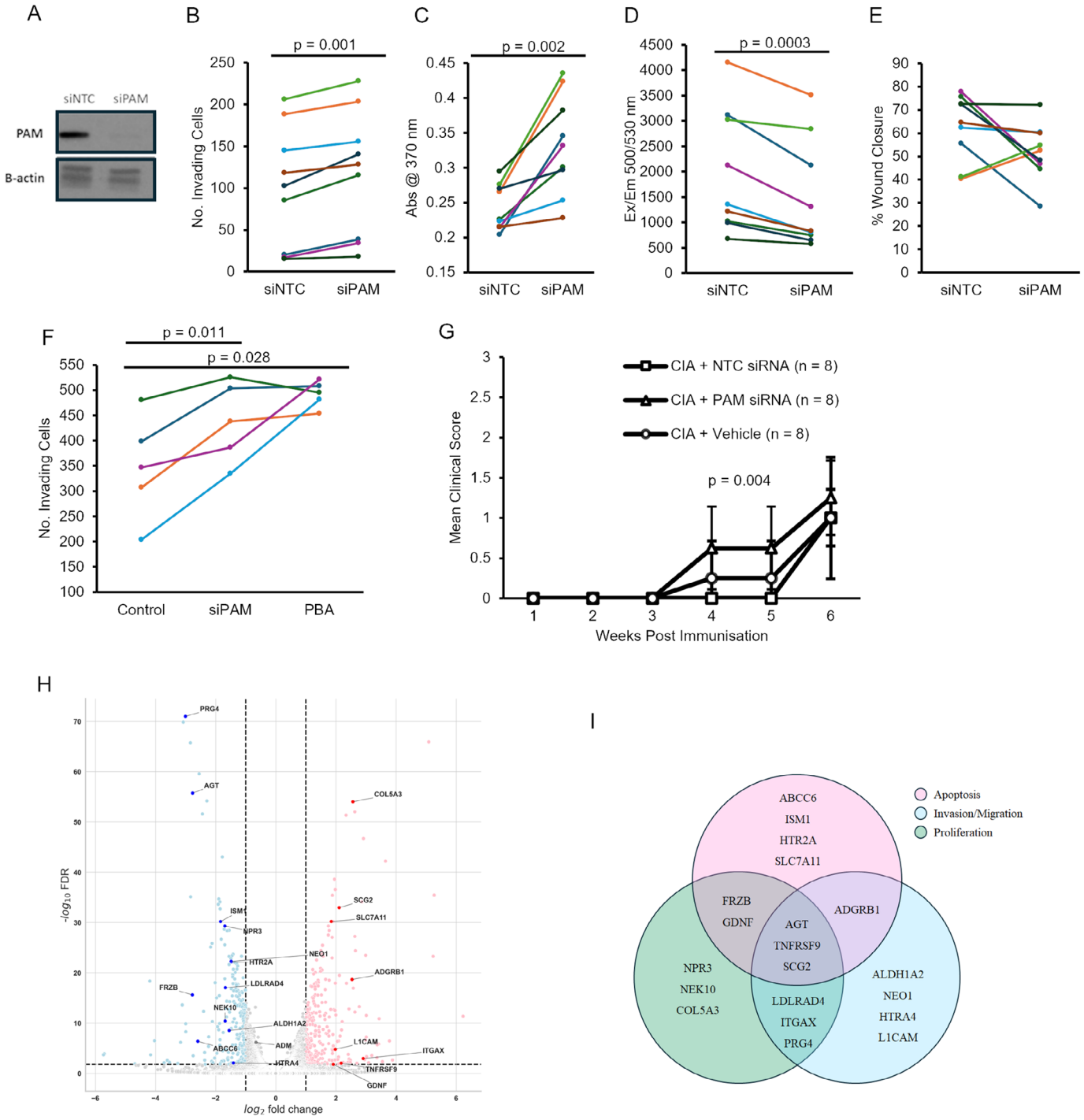

Figure 2. Effects of peptidylglycine alpha-amidating monooxygenase (PAM) inhibition on rheumatoid arthritis synovial fibroblast (RASF) biology. (A) Western blot demonstrating 92% reduction of PAM in RASFs following small interfering RNA targeting PAM (siPAM) treatment compared to nontargeting control small interfering RNA (siNTC). RASFs treated with siPAM showed significantly higher (B) proliferation, (C) invasion, and (D) lower apoptosis compared to RASFs treated with siNTC in n = 9 cell lines. (E) Migration rate was unaffected. (F) Inhibition of PAM enzymatic activity increased invasiveness in n = 5 cell lines, similar to treatment with siPAM. (G) Small interfering RNA (siRNA) knockdown of PAM in the collagen-induced arthritis (CIA) model increased clinical activity score at weeks 4 and 5 compared to mice treated with NTC (n = 8 each). (H) Volcano plot of RNA sequencing data from RASFs after siPAM treatment revealed differential expression of genes involved in (I) proliferation, invasion, and apoptosis pathways compared with siNTC. FDR, false discovery rate; No., number; PBA, 4-phenyl-3-butenoic acid.

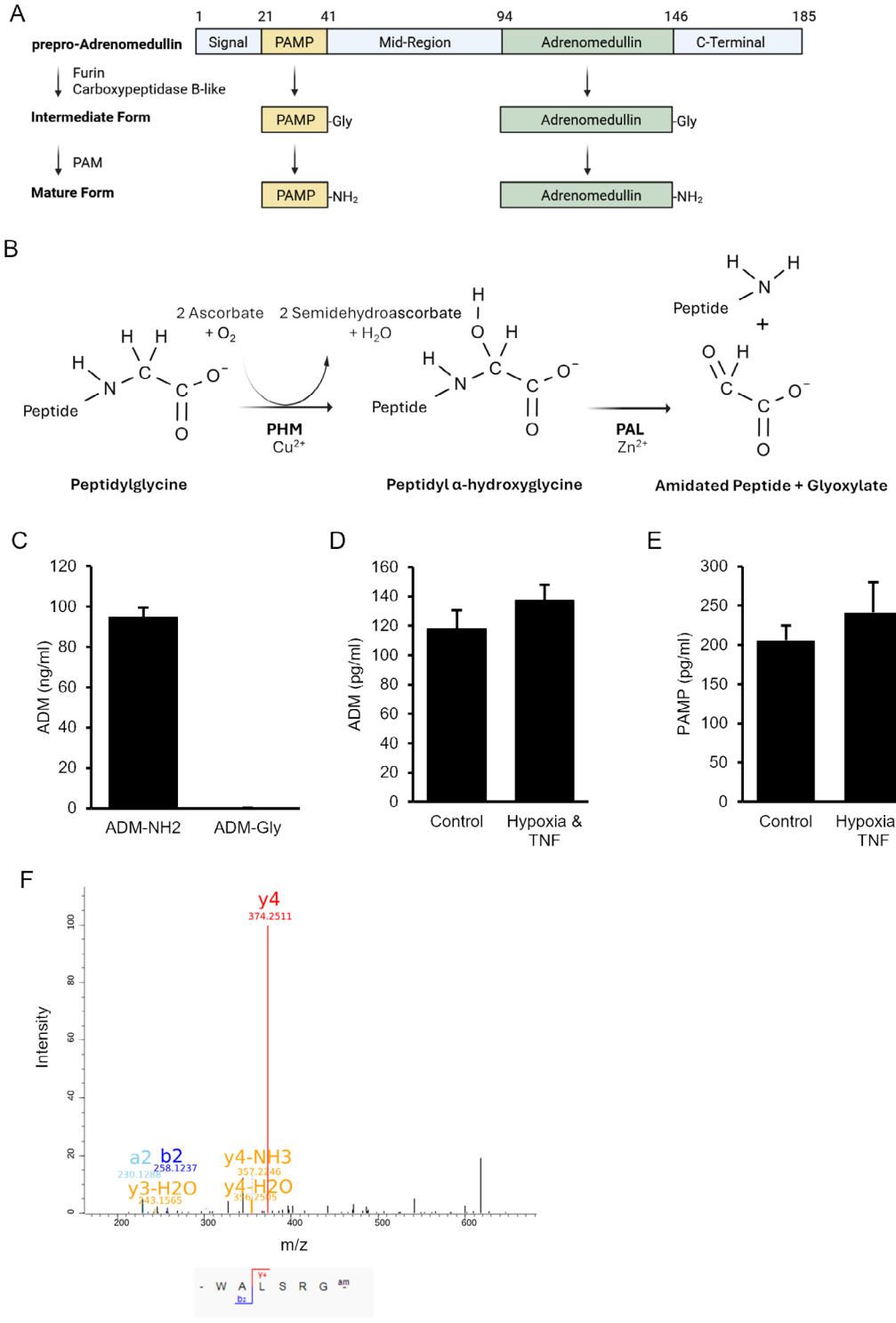

Figure 3. Identification of amidated peptides in rheumatoid arthritis synovial fibroblast (RASF) secretome. (A) Processing of preproadrenomedullin (ADM) into amidated ADM (ADM-NH_2) and amidated pro-ADM N-terminal peptide (PAMP-NH_2). (B) Amidation of peptidylglycine substrates by peptidylglycine alpha-amidating monooxygenase (PAM). (C) ADM enzyme-linked immunosorbent assay (ELISA) is specific for ADM-NH_2 using ADM-NH_2 and glycine-extended ADM (ADM-Gly) peptides. (D) Detection of ADM-NH_2 in RASF supernatants (n = 3) via ELISA in control and hypoxia/tumor necrosis factor (TNF) conditions. (E) Detection of total PAMP in RASF supernatants (n = 3) via ELISA in control and hypoxia/TNF conditions. (F) Mass spectrometry/mass spectrometry spectra of PAMP-NH_2 detected in RASF supernatant. PAL, peptidylglycine amidoglycolate lyase; PAMP-Gly, glycine-extended PAMP; PHM, peptidyl alpha-hydroxylating monooxygenase.

$CD86^-/CD206^+$ (M2) to $CD86^+/CD206^-$ (M1).[3] Loss-of-function mutations in *PRG4* cause an autosomal recessive condition that includes synovial hyperplasia, joint swelling, and damage.[19]

RASFs secrete amidated peptides, including ADM and PAMP. Because amidation is an underlying mechanism regulating RASF invasiveness, it was important to identify the amidated proteome of RASFs. Transcriptomic analysis revealed several preprohormone peptides that are expressed in RASFs (Supplementary Data Table 5). The highest expressed was *ADM*, which encodes two peptides that are both amidated: ADM and PAMP. *ADM* was significantly down-regulated in siPAM-treated RASFs compared to siNTC (FDR $P = 6.63^{-7}$).

Prepro-ADM is processed posttranslationally by the prohormone convertase furin and a carboxypeptidase B-type enzyme to produce ADM and PAMP[20] (Figure 3A). PAM then carries out amidation by conversion of the penultimate residue of the peptidylglycine substrate into an alpha amide. The peptidyl alpha-hydroxylating monooxygenase domain catalyzes the hydroxylation of the alpha carbon, followed by the peptidylglycine amidoglycolate lyase domain cleaving the N-C-alpha bond to produce an alpha-amidated peptide and glyoxylate[21] (Figure 3B). Amidation is oxygen dependent, and PAM is induced by hypoxia (Supplementary Data Figure 4A and B), which allows PAM to function in the low-oxygen environment of the RA joint. This is demonstrated by the detection of ADM-NH_2 in the RASF secretome under hypoxic conditions (Supplementary Data Figure 4C).

Specificity of the ADM ELISA for ADM-NH_2 was confirmed by using peptides, which demonstrate detection of ADM-NH_2 only (Figure 3C). ADM-NH_2 secretion from RASFs was confirmed by ELISA and was not influenced by either hypoxia or TNFα (Figure 3D). Total PAMP secretion was measured by ELISA, with hypoxia and TNFα having no effect (Figure 3E). PAMP-NH_2 secretion was confirmed using mass spectroscopy (Figure 3F).

ADM-NH_2 and PAMP-NH_2 inhibit RASF inflammatory cytokine production and invasiveness. ADM is a signaling peptide with anti-inflammatory effects on an RA animal model[22] and has shown efficacy in early-stage therapeutic trials of inflammatory bowel diseases.[23] Little is known about the biologic activities of PAMP in inflammation. Peptide amidation has been shown to increase half-life and receptor affinity.[24] We used an in vitro assay to measure half-life; this revealed ADM-NH_2 to have a significantly longer half-life than ADM-Gly; 21 versus 10.9 hours, respectively (Figure 4A and B). Additionally, ADM-NH_2 has been reported to bind its cognate receptor with 40-fold greater affinity compared with ADM-Gly.[25] Amidation of ADM therefore results in greater bioactivity.

We next compared the effects of amidated and non–ADM-NH_2 and PAMP-NH_2 on TNFα-induced inflammatory cytokine production by RASFs; incubation with both forms of PAMP inhibited IL-6 production, with PAMP-NH_2 being more potent (–30%, $P = 0.047$); ADM variants did not have an effect (Figure 4C). Similarly, both versions of PAMP inhibited IL-8 production, with PAMP-NH_2 having a greater effect (–23%, $P = 0.02$; Figure 4D). The invasiveness of RASFs was reduced upon incubation with ADM-NH_2 (–19%, $P = 0.03$) and PAMP-NH_2 (–30%, $P = 0.036$) compared to their glycine-extended precursors; culture with both peptides resulted in greater reduction than either alone (–38%, $P = 0.043$; Figure 4E).

ADM-NH_2 induces expression of PRG4 via TGFβ reducing RASF tissue–damaging activities. The reduction of *PRG4* expression following PAM inhibition was intriguing given the formers critical role in joint homeostasis[26] and inflammation.[3] The therapeutic benefits of ADM-NH_2 administration to models of RA[27] and inflammatory bowel diseases[28,29] have been linked with up-regulation of TGFβ production. *PRG4* expression is up-regulated by TGFβ and inhibited by IL-1 and TNFα.[30] We hypothesized that ADM-NH_2 may induce higher *PRG4* via TFGβ, resulting in altered RASF-associated tissue-damaging activities. Incubation of RASFs with ADM-NH_2 and PAMP-NH_2 resulted in significantly greater TGFβ than culture with glycine-extended versions (ADM-NH_2 +86%, $P = 0.023$; PAMP-NH_2 +38%, $P = 0.037$; Figure 5A). We next determined the effect of PRG4 on RASF activities using siRNA (Figure 5B). RASFs transfected with siPRG4 (n = 5) displayed greater invasiveness (+118%, $P = 0.003$) (Figure 5C) and proliferation (+7%, $P = 0.03$; Figure 5D), whereas apoptosis was reduced (–13%, $P = 0.048$; Figure 5D) compared to siNTC-exposed cells; migration was not significantly changed (Figure 5F). These results are broadly similar to those resulting from *PAM* inhibition (Figure 2B–E).

Inhibition of amidation shifts macrophages toward a proinflammatory state. Signals from RASFs can modulate synovial macrophage polarization and disease activity.[31] To determine the role of amidation in mediating macrophage polarity, we used an RASF–macrophage coculture model and PBA. Inhibition of amidation increased M1 macrophages ($MerTK^-CD48^+$ [+29%, $P = 0.001$] and $MerTK^-CD86^+$ [+31%, $P = 0.001$]; Figure 6A and B, respectively) and decreased M2 macrophages ($MerTK^+CD86^-$ [–32%, $P = 0.004$], $MerTK^+CD48^+$ [–12%, $P = 0.001$], and $MerTK^+CD86^+$ [–11%, $P = 0.002$] compared to control; Figure 6C–E). Incubation of macrophages alone with PBA had no effect on polarization (Supplementary Data Figure 5), indicating that the effect is mediated by a secreted amidated product of RASFs.

We next determined whether ADM and PAMP had effects on the release of proinflammatory cytokines by LPS-induced macrophages (Figure 6F and G). Compared to control, ADM-NH_2 reduced secretion of IL-8 (–55%, $P = 0.011$) and TNFα

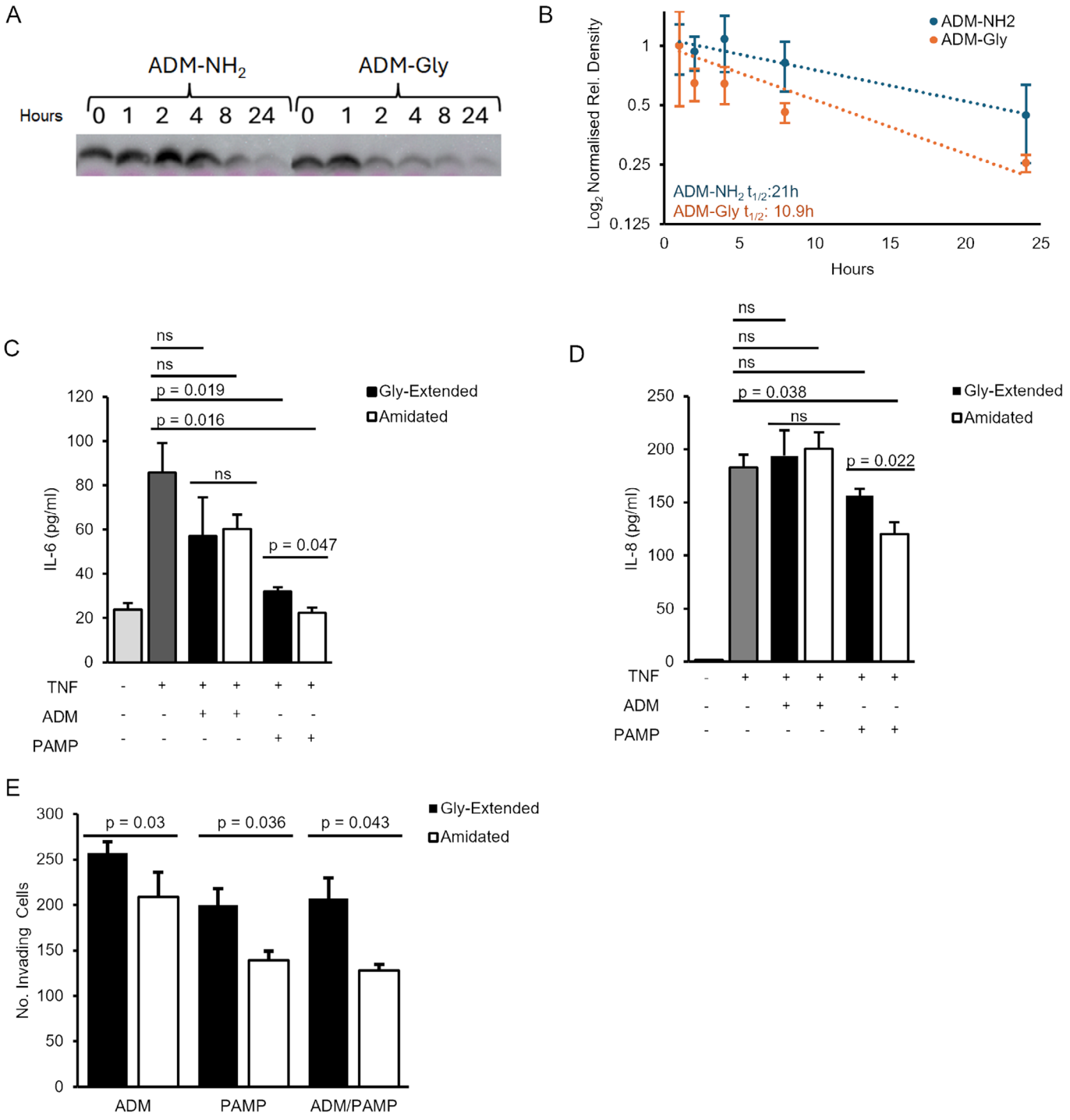

Figure 4. Amidated adrenomedullin (ADM-NH_2) and amidated pro-ADM N-terminal peptide (PAMP-NH_2) inhibit rheumatoid arthritis synovial fibroblast (RASF) inflammatory cytokine production and invasiveness. (A) Western blot and (B) ADM-NH_2 and glycine-extended ADM (ADM-Gly) degradation time course, ADM-NH_2 half-life is 21 hours (h), ADM-Gly half-life is 10.9 h. RASFs were incubated with tumor necrosis factor (TNF) and ADM or PAMP peptides. (C) Interleukin-6 (IL-6) production was reduced by PAMP-NH_2 and glycine-extended PAMP (PAMP-Gly), with the former having a greater effect. (D) IL-8 production was not altered by either form of ADM, only PAMP-NH_2 had a significant effect. (E) Amidated peptides had greater suppressive effects on RASF invasiveness compared with glycine-extended peptides. No., number; ns, not significant; Rel., relative.

(–47%, P = 0.002), whereas ADM-Gly had no significant impact for either cytokine compared to control. ADM-NH_2 reduced IL-8 (–42%, P = 0.032) and TNFα (–43%, P = 0.024) compared to ADM-Gly. Both PAMP-NH_2 (–37%, P = 0.04) and PAMP-Gly (–42%, P = 0.032) reduced IL-8 secretion compared to control, whereas only PAMP-Gly (–27%, P = 0.015) reduced TNFα

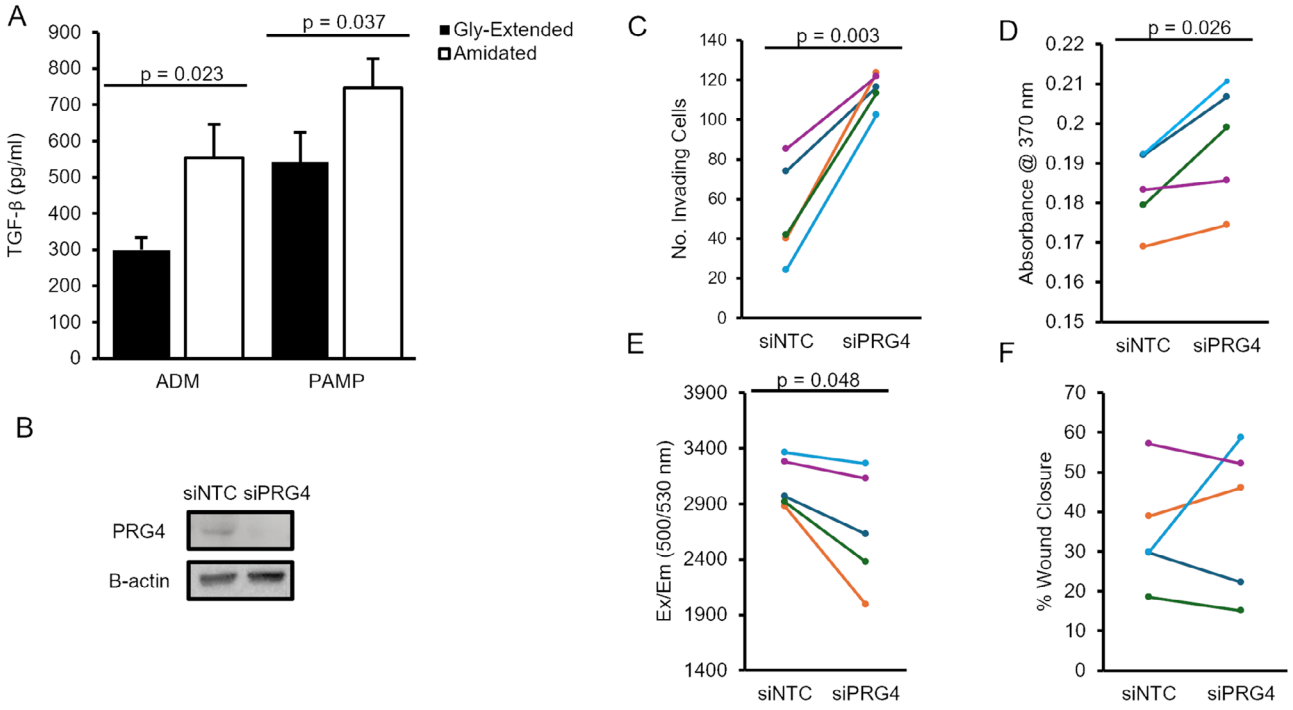

Figure 5. Amidated adrenomedullin (ADM-NH_2) and amidated pro-ADM N-terminal peptide (PAMP-NH_2) induce expression PRG4 via transforming growth factor β (TGFβ), resulting in reduced rheumatoid arthritis synovial fibroblast (RASF) tissue–damaging activities. (A) TGFβ secretion is higher in tumor necrosis factor–stimulated RASFs exposed to ADM-NH_2 or PAMP-NH_2 compared with glycine (Gly)-extended peptides. (B) RASF PRG4 protein levels are reduced by small interfering RNA targeting PRG4 (siPRG4) treatment compared to nontargeting control small interfering RNA (siNTC). Inhibition of PRG4 leads to significantly greater (C) proliferation, (D) invasion, (E) lower apoptosis, and (F) no significant difference in migration compared to RASFs treated with siNTC in n = 5 cell lines. Ex/Em, excitation/emission; No., number.

secretion compared to control. There was no significant difference observed between PAMP-NH_2 and PAMP-Gly on IL-8 or TNFα secretion.

DISCUSSION

Our data reveal the RA susceptibility and severity associated variant rs26232 to be an eQTL for *PAM*, with the risk C allele linked with low expression in RASFs. The resultant reduced levels of ADM-NH_2 and PAMP-NH_2 increase the inflammatory and tissue damage activities of RASFs and drive macrophages to proinflammatory subtypes. We show that the downstream effect on RASFs is influenced by TGFβ-induced PRG4 activity.

PAM has critical functions in the posttranslational modification of inactive peptidylglycine precursors to bioactive alpha-amidated peptides and is mainly present in the secretory pathway.[32] Ablation of *PAM* is embryonically lethal; heterozygote knockout mice have behavioral and metabolic defects.[16] It has roles in cytoskeletal organization as a secretagogue and in modulating gene expression.[33] Expression of *PAM* has similar sensitivity to hypoxia as hypoxia-inducible factor hydroxylases, whereas the activity of the PHL domain of PAM is oxygen dependent and falls linearly from 10% to 0% O_2.[34] Despite the RA synovium being hypoxic with O_2 of 3%,[35] we detected peptide amidation occurring in RASFs cultured in these conditions.

The invasive activities of RASFs in vitro are positively correlated with the rate of radiologically assessed joint damage over subsequent years.[5] The rs26232 C variant is associated with greater radiologic damage, and RASFs of this genotype are more invasive and express higher levels of chemokines and adhesion molecules.[11] Our data are consistent with a model in which lower amidation of ADM and PAMP results in increased inflammatory cytokine production and invasiveness of RASFs, and this is related to lower TGFβ-induced *PRG4* production. PRG4 is a key regulator of synovial joint homeostasis, having both important mechanical and anti-inflammatory effects.[26]

AMP2 data demonstrate that PAM expression is significantly higher in RASFs compared to all other cell types in the synovium. This suggests that RASFs are the most important source of amidated peptides in the RA synovium, though the study of other synovial cell types, particularly endothelial, is warranted. Although *PAM* is not expressed in immune cells, by using an RASF–macrophage coculture model, we found that pharmacological inhibition with PBA increased polarization toward proinflammatory $MerTK^-CD48^+$ and $MerTK^-CD86^+$ macrophages and reduced anti-inflammatory $MerTK^+CD48^+$, $MerTK^+CD86^+$, and $MerTK^+CD86^-$ macrophages. $MerTK^+$ macrophages are

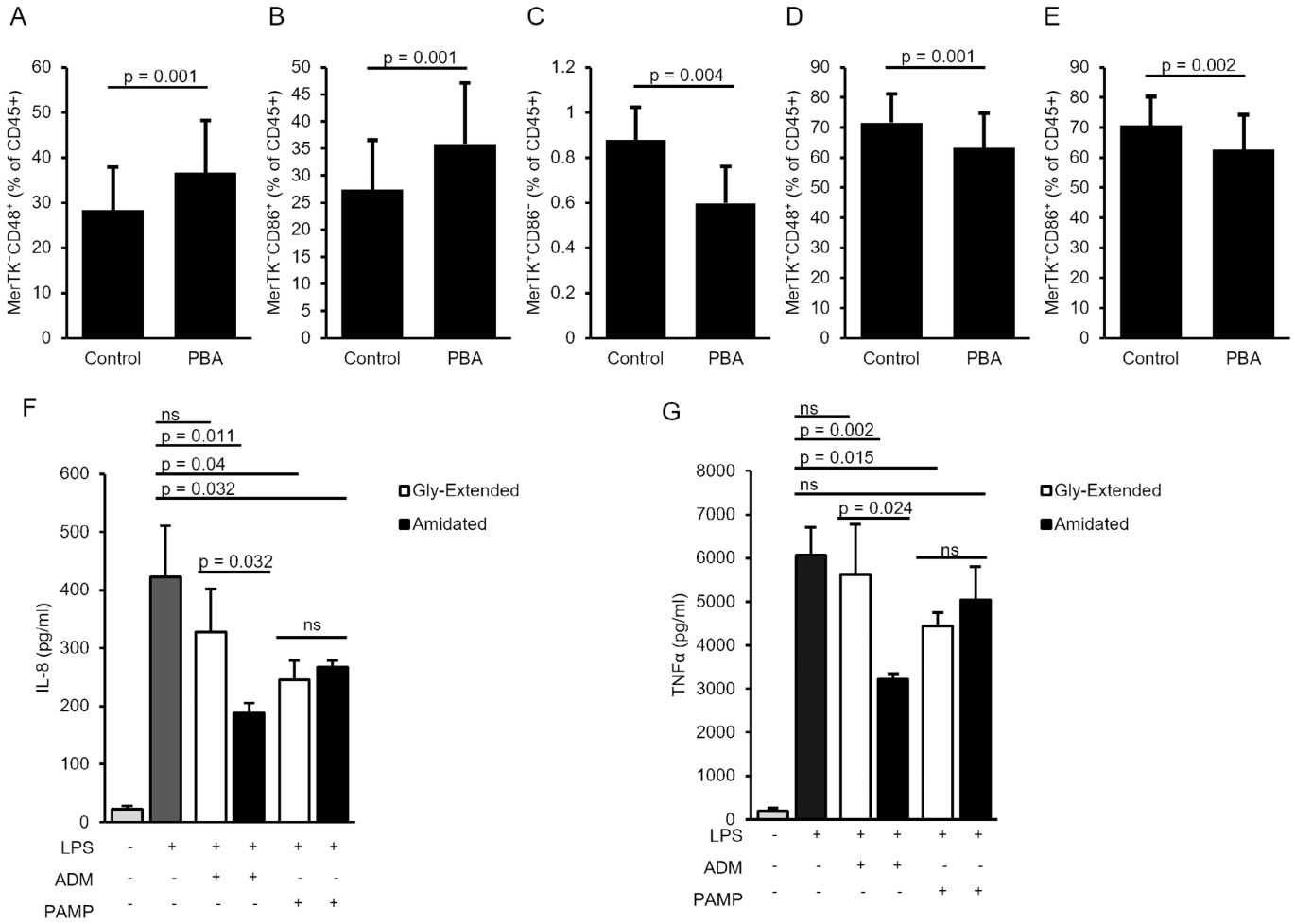

Figure 6. Inhibition of amidation in rheumatoid arthritis synovial fibroblasts (RASFs) results in a shift from M2 to M1 macrophages. Flow cytometry data demonstrating an increase in (A) MerTK$^-$CD48$^+$ and (B) MerTK$^-$CD86$^+$ macrophages and decrease in (C) MerTK$^+$CD86$^-$, (D) MerTK$^+$CD48$^+$, and (E) MerTK$^+$CD86$^+$ macrophages in RASF–macrophage cocultures incubated with 4-phenyl-3-butenoic acid (PBA). Macrophages were incubated with lipopolysaccharide (LPS) and adrenomedullin (ADM) or pro-ADM N-terminal peptide (PAMP) peptides. (F) Interleukin-8 (IL-8) production was reduced by amidated ADM (ADM-NH_2), but not glycine (Gly)-extended ADM, and by amidated PAMP and Gly-extended PAMP (PAMP-Gly). (G) Tumor necrosis factor (TNF) production was reduced by ADM-NH_2 and PAMP-Gly only. ns, not significant.

enriched in healthy controls/RA remission and are associated with lower disease activity and inflammation markers. MerTK$^-$ macrophages are enriched in patients with active RA and are associated with higher disease activity and inflammation markers.[31] In this way, genetically determined decreased levels of *PAM* can shift macrophages toward a proinflammatory population, which increases inflammation and disease severity. In the RASF secretome, ADM is the most highly expressed amidated peptide. These data are consistent with data showing that administration of ADM to an animal model of uveitis resulted in decreased inflammation, greater TGFβ expression, and a shift to M2 macrophages.[36]

Our data complement GWAS in several other common human diseases; susceptibility to Parkinson disease (PD) is associated with rs26431 C allele,[37] which is in LD with rs26232 C (D' = 0.73, r^2 = 0.53 in 1,000 genomes european cohort), and primary biliary cirrhosis (PBC) is associated with the rs526231 C allele,[38] which is also in LD with rs26232 C (D' = 0.92, r^2 = 0.84 in 1,000 genomes european cohort). GTEx data reveal *PAM* to be highly expressed in the brain but minimally in the liver, perhaps implicating a low-frequency cell type in the pathogenesis of PBC or the effect of an amidated peptide produced extrahepatically. Low-frequency nonsynonymous *PAM* variants have been associated with risk of type 2 diabetes, which is attributed to reduced amidation of chromogranin A, leading to lower insulin secretion by pancreatic β cells.[39] Characterizing the amidated proteome of disease-relevant tissues in PD and PBC may reveal the mechanisms by which low PAM activity contributes to the pathogenesis of these conditions.

Our data reveal an important new mechanism regulating fibroblast-mediated tissue damage in RA, representing the first known role for PAM in both RA and fibroblast biology. We also

demonstrate the impact of amidated peptides on macrophages, showing that PAM has an effect beyond fibroblasts in RA. Most of the recent advances in RA treatment have targeted immune cells; although highly clinically effective, the resulting immunosuppression increases the risk of infection.[40] This risk is believed to be lower using treatments centered on fibroblasts. Therapies based on systemic administration of amidated proteins, such as ADM and PAMP, may be effective in RA with the added potential of using rs26232 genotype to preidentify patients most likely to benefit from such agents.

ACKNOWLEDGMENTS

We are grateful to our late colleague Professor Douglas Veale for access to synovial biopsy samples. We thank our patient and public Research Advisory Panel for input throughout the study. We would like to thank Dr Alison Gartland (University of Sheffield) because the animal component was conducted on her Home Office project license.

AUTHOR CONTRIBUTIONS

All authors contributed to at least one of the following manuscript preparation roles: conceptualization AND/OR methodology, software, investigation, formal analysis, data curation, visualization, and validation AND drafting or reviewing/editing the final draft. As corresponding author, Dr Sheridan confirms that all authors have provided the final approval of the version to be published, and takes responsibility for the affirmations regarding article submission (eg, not under consideration by another journal), the integrity of the data presented, and the statements regarding compliance with institutional review board/Declaration of Helsinki requirements. All authors contributed to the investigation, formal analysis of the data, and writing, reviewing, and editing of the manuscript.

REFERENCES

1. Knevel R, Gröndal G, Huizinga TW, et al. Genetic predisposition of the severity of joint destruction in rheumatoid arthritis: a population-based study. Ann Rheum Dis 2012;71(5):707–709. doi:https://doi.org/10.1136/annrheumdis-2011-200627
2. Walsh AM, Whitaker JW, Huang CC, et al. Integrative genomic deconvolution of rheumatoid arthritis GWAS loci into gene and cell type associations. Genome Biol 2016;17(1):79. doi:https://doi.org/10.1186/s13059-016-0948-6
3. Qadri M, Jay GD, Zhang LX, et al. Proteoglycan-4 is an essential regulator of synovial macrophage polarization and inflammatory macrophage joint infiltration. Arthritis Res Ther 2021;23(1):241. doi:https://doi.org/10.1186/s13075-021-02621-9 Erratum in: Arthritis Res Ther 2021;23:276.
4. Lefèvre S, Knedla A, Tennie C, et al. Synovial fibroblasts spread rheumatoid arthritis to unaffected joints. Nat Med 2009;15(12):1414–1420. doi:https://doi.org/10.1038/nm.2050
5. Tolboom TC, van der Helm-Van Mil AH, Nelissen RG, et al. Invasiveness of fibroblast-like synoviocytes is an individual patient characteristic associated with the rate of joint destruction in patients with rheumatoid arthritis. Arthritis Rheum 2005;52(7):1999–2002. doi:https://doi.org/10.1002/art.21118
6. Stahl EA, Raychaudhuri S, Remmers EF, et al; BIRAC Consortium; YEAR Consortium. Genome-wide association study meta-analysis identifies seven new rheumatoid arthritis risk loci. Nat Genet 2010;42(6):508–514. doi:https://doi.org/10.1038/ng.582
7. Viatte S, Plant D, Bowes J, et al. Genetic markers of rheumatoid arthritis susceptibility in anti-citrullinated peptide antibody negative patients. Ann Rheum Dis 2012;71(12):1984–1990. doi:https://doi.org/10.1136/annrheumdis-2011-201225
8. Teare MD, Knevel R, Morgan MD, et al. Allele-dose association of the C5orf30 rs26232 variant with joint damage in rheumatoid arthritis. Arthritis Rheum 2013;65(10):2555–2561. doi:https://doi.org/10.1002/art.38064
9. Muthana M, Hawtree S, Wilshaw A, et al. C5orf30 is a negative regulator of tissue damage in rheumatoid arthritis. Proc Natl Acad Sci U S A 2015;112(37):11618–11623. doi:https://doi.org/10.1073/pnas.1501947112
10. Dorris ER, Tazzyman SJ, Moylett J, et al. The autoimmune susceptibility gene *C5orf30* regulates macrophage-mediated resolution of inflammation. J Immunol 2019;202(4):1069–1078. doi:https://doi.org/10.4049/jimmunol.1801155
11. Dorris ER, Linehan E, Trenkmann M, et al. Association of the rheumatoid arthritis severity variant rs26232 with the invasive activity of synovial fibroblasts. Cells 2019;8(10):1300. doi:https://doi.org/10.3390/cells8101300
12. Lewis MJ, Barnes MR, Blighe K, et al. Molecular portraits of early rheumatoid arthritis identify clinical and treatment response phenotypes. Cell Reports 2017;28(9): 2455-2470.e5. https://doi.org/10.1016/j.celrep.2019.07.091
13. Zhang F, Jonsson AH, Nathan A, et al; Accelerating Medicines Partnership: RA/SLE Network. Deconstruction of rheumatoid arthritis synovium defines inflammatory subtypes. Nature 2023;623(7987):616–624. doi:https://doi.org/10.1038/s41586-023-06708-y
14. Robinson MD, McCarthy DJ, Smyth GK. edgeR: a Bioconductor package for differential expression analysis of digital gene expression data. Bioinformatics 2010;26(1):139–140. doi:https://doi.org/10.1093/bioinformatics/btp616
15. Mueller GP, Driscoll WJ, Eipper BA. In vivo inhibition of peptidylglycine-alpha-hydroxylating monooxygenase by 4-phenyl-3-butenoic acid. J Pharmacol Exp Ther 1999;290(3):1331–1336. doi:https://doi.org/10.1016/S0022-3565(24)35039-6
16. Gaier ED, Eipper BA, Mains RE. Pam heterozygous mice reveal essential role for Cu in amygdalar behavioral and synaptic function. Ann N Y Acad Sci 2014;1314(1):15–23. doi:https://doi.org/10.1111/nyas.12378
17. Coles JM, Zhang L, Blum JJ, et al. Loss of cartilage structure, stiffness, and frictional properties in mice lacking PRG4. Arthritis Rheum 2010;62(6):1666–1674. doi:https://doi.org/10.1002/art.27436
18. Al-Sharif A, Jamal M, Zhang LX, et al. Lubricin/proteoglycan 4 binding to CD44 receptor: a mechanism of the suppression of proinflammatory cytokine-induced synoviocyte proliferation by lubricin. Arthritis Rheumatol 2015;67(6):1503–1513. doi:https://doi.org/10.1002/art.39087
19. Marcelino J, Carpten JD, Suwairi WM, et al. CACP, encoding a secreted proteoglycan, is mutated in camptodactyly-arthropathy-coxa vara-pericarditis syndrome. Nat Genet 1999;23(3):319–322. doi:https://doi.org/10.1038/15496
20. Kim W, Essalmani R, Szumska D, et al. Loss of endothelial furin leads to cardiac malformation and early postnatal death. Mol Cell Biol 2012;32(17):3382–3391. doi:https://doi.org/10.1128/MCB.06331-11
21. Prigge ST, Kolhekar AS, Eipper BA, et al. Amidation of bioactive peptides: the structure of peptidylglycine alpha-hydroxylating monooxygenase. Science 1997;278(5341):1300–1305. doi:https://doi.org/10.1126/science.278.5341.1300
22. Ah Kioon M-D, Asensio C, Ea H-K, et al. Adrenomedullin(22-52) combats inflammation and prevents systemic bone loss in murine collagen-induced arthritis. Arthritis Rheum 2012;64(4):1069–1081. doi:https://doi.org/10.1002/art.33426

23. Kita T, Ashizuka S, Takeda T, et al. Adrenomedullin for biologic-resistant Crohn's disease: a randomized, double-blind, placebo-controlled phase 2a clinical trial. J Gastroenterol Hepatol 2022; 37(11):2051–2059. doi:https://doi.org/10.1111/jgh.15945
24. Wettergren A, Pridal L, Wøjdemann M, et al. Amidated and non-amidated glucagon-like peptide-1 (GLP-1): non-pancreatic effects (cephalic phase acid secretion) and stability in plasma in humans. Regul Pept 1998;77(1-3):83–87. doi:https://doi.org/10.1016/S0167-0115(98)00044-5
25. Eguchi S, Hirata Y, Iwasaki H, et al. Structure-activity relationship of adrenomedullin, a novel vasodilatory peptide, in cultured rat vascular smooth muscle cells. Endocrinology 1994;135(6):2454–2458. doi: https://doi.org/10.1210/endo.135.6.7988431
26. Maenohara Y, Chijimatsu R, Tachibana N, et al. Lubricin contributes to homeostasis of articular cartilage by modulating differentiation of superficial zone cells. J Bone Miner Res 2021;36(4):792–802. doi: https://doi.org/10.1002/jbmr.4226
27. Gonzalez-Rey E, Chorny A, O'Valle F, et al. Adrenomedullin protects from experimental arthritis by down-regulating inflammation and Th1 response and inducing regulatory T cells. Am J Pathol 2007;170(1): 263–271. doi:https://doi.org/10.2353/ajpath.2007.060596
28. Ashizuka S, Inagaki-Ohara K, Kuwasako K, et al. Adrenomedullin treatment reduces intestinal inflammation and maintains epithelial barrier function in mice administered dextran sulphate sodium. Microbiol Immunol 2009;53(10):573–581. doi:https://doi.org/10.1111/j.1348-0421.2009.00159.x
29. Gonzalez-Rey E, Chorny A, Varela N, et al. Urocortin and adrenomedullin prevent lethal endotoxemia by down-regulating the inflammatory response. Am J Pathol 2006;168(6):1921–1930. doi:https://doi.org/10.2353/ajpath.2006.051104
30. Jones AR, Flannery CR. Bioregulation of lubricin expression by growth factors and cytokines. Eur Cell Mater 2007;13:40–45. doi: https://doi.org/10.22203/eCM.v013a04
31. Alivernini S, MacDonald L, Elmesmari A, et al. Distinct synovial tissue macrophage subsets regulate inflammation and remission in rheumatoid arthritis. Nat Med 2020;26(8):1295–1306. doi:https://doi.org/10.1038/s41591-020-0939-8
32. Lindberg I, Glembotski CC. Physiological signaling in the absence of amidated peptides. Proc Natl Acad Sci U S A 2019;116(40):19774–19776. doi:https://doi.org/10.1073/pnas.1914001116
33. Francone VP, Ifrim MF, Rajagopal C, et al. Signaling from the secretory granule to the nucleus: Uhmk1 and PAM. Mol Endocrinol 2010;24(8): 1543–1558. doi:https://doi.org/10.1210/me.2009-0381
34. Simpson PD, Eipper BA, Katz MJ, et al. Striking oxygen sensitivity of the peptidylglycine α-amidating monooxygenase (PAM) in neuroendocrine cells. J Biol Chem 2015;290(41):24891–24901. doi:https://doi.org/10.1074/jbc.M115.667246
35. Ng CT, Biniecka M, Kennedy A, et al. Synovial tissue hypoxia and inflammation in vivo. Ann Rheum Dis 2010;69(7):1389–1395. doi: https://doi.org/10.1136/ard.2009.119776
36. Matsuda Y, Tanaka M, Zhao Y, et al. Adrenomedullin-RAMP2 system modulates inflammation and tissue repair in experimental autoimmune uveitis via T-cell and M2 macrophage regulation. Invest Ophthalmol Vis Sci 2025;66(6):12. doi:https://doi.org/10.1167/iovs.66.6.12
37. Nalls MA, Blauwendraat C, Vallerga CL, et al; 23andMe Research Team; System Genomics of Parkinson's Disease Consortium; International Parkinson's Disease Genomics Consortium. Identification of novel risk loci, causal insights, and heritable risk for Parkinson's disease: a meta-analysis of genome-wide association studies. Lancet Neurol 2019;18(12):1091–1102. doi:https://doi.org/10.1016/S1474-4422(19)30320-5
38. Cordell HJ, Han Y, Mells GF, et al; Canadian-US PBC Consortium; Italian PBC Genetics Study Group; UK-PBC Consortium. International genome-wide meta-analysis identifies new primary biliary cirrhosis risk loci and targetable pathogenic pathways. Nat Commun 2015; 6(1):8019. doi:https://doi.org/10.1038/ncomms9019
39. Thomsen SK, Raimondo A, Hastoy B, et al. Type 2 diabetes risk alleles in PAM impact insulin release from human pancreatic β-cells. Nat Genet 2018;50(8):1122–1131. doi:https://doi.org/10.1038/s41588-018-0173-1
40. Jones DS, Jenney AP, Swantek JL, et al. Profiling drugs for rheumatoid arthritis that inhibit synovial fibroblast activation. Nat Chem Biol 2017;13(1):38–45. doi:https://doi.org/10.1038/nchembio.2211